PHYSICAL REVIEW B VOLUME 24, NUMBER 10 15 NOVEMBER 1981

Metal-nonmetal transition in Cs-Xe mixtures

R. D. Swenumson,* S. Leutwyler, and U. Even
Chemistry Department, Tel-Aviv University, Tel Aviv, Israel
(Received 21 November 1980)

Electrical transport and optical data on amorphous-metal—rare-gas mixtures of Cs-Xe at 6 K are presented. The Cs-Xe mixtures fit a model whereby most of the Cs is distributed randomly on the microscopic scale while a small amount exists in the form of granular clusters. Although preferential clustering occurs, it is not prominent enough to apply the model of classical percolation theory to the metal-nonmetal transition which is exhibited. The transition is located at 0.55 ± 0.01 Cs atomic fraction based upon the closure of the optical gap and the threshold of extended-state conduction. The composition range over which the states at the Fermi energy are localized is very small or zero.

I. INTRODUCTION

The study of metals mixed with rare gases at liquid-He temperatures is extensive.[1–5] Optical and electrical transport measurements have been performed on many combinations of metallic elements with all noble gases. The scope of optical studies range from investigating crystal-field splitting of very dilute matrix isolated metallic atoms[6] to the study of the metal-nonmetal transition (MNMT).[1–5,7]

A material exhibiting an MNMT is transformed by means of an externally controlled parameter such as pressure,[8,9] temperature,[10] magnetic field,[11] or composition[1–5,12–14] from a nonmetallic state to a metallic state. An MNMT is observed in expanded liquid metals[8,9] such as Hg and Cs, by changing the liquid density with high-temperature and high-pressure techniques.

The preparation of metal—noble-gas mixtures is a convenient means of controllably changing the metallic density from dilute compositions in which the mixture has nonmetallic optical and electrical transport properties, to dense metallic compositions in which metallic properties are exhibited. The inherent assumption in this method of density expansion is a weak influence of the van der Waals bonded rare-gas matrix on the physical properties of the expanded metal. The advantage of investigating expanded metals with this technique is that the effects of high temperature which tend to obscure interesting physical features are absent. The metal-nonmetal transition in amorphous mixtures of Cs and Xe was the subject of the present investigation.

II. EXPERIMENTAL APPARATUS

A. Molecular beam sources

The mixtures are prepared by direct codeposition of the two components, Cs and Xe, on a 6 K sapphire substrate. Each molecular beam is flagged separately, enabling independent beam switching.

Xenon (99.995% pure) was released from a gas cylinder into a baked and evacuated reservoir (~ 1 liter) until a pressure of 100 Torr was achieved. A leak valve (Vacuum Generators, MD6) isolated the Xe reservoir from the tube which served as the gas duct to the point where it was released into the ultrahigh vacuum (UHV) chamber. The direct deposition rates were calibrated by monitoring the intensity interference oscillations of monochromatized light ($\lambda = 689$ nm) transmitted through the Xe film as its thickness increased during deposition onto the sample substrate. The interference effect is determined from the relation $R = \lambda/(2nt)$, where R is the time rate of thickness increase of the Xe deposited on the sample window, λ is the photon wavelength, n is the index of refraction of Xe (1.3),[15] and t is the oscillation period. Each absolute deposition rate was simultaneously correlated with the background Xe pressure (determined by a Vacuum Generator VIG 20 ionization gauge) as well as the numerical indication on the leak valve scale.

The absolute accuracy of the ionization gauge calibration was 5% as determined from several attempts to reproduce a certain Xe deposition rate from the ionization gauge indication. Deposition rates resulting from indirect deposition due to the background pressure of Xe were measured to be about 10% of the direct rates. Short-(1-sec) and long-(30-min) term deposition rate stabilities indicated by the ionization gauge were better than 2%. The range of the calibrated rates was $0.4-5$ Å sec^{-1} and the corresponding Xe pressure range was 3×10^{-6} to 10^{-4} Torr.

The Cs molecular beam source is a reflux-type, temperature-stabilized oven which collects and recirculates the unused (off-axis) part of the beam. The design and operation of the beam source is described elsewhere.[16] The Cs deposition rate, as calibrated with a quartz crystal thickness monitor indicated an absolute rate accuracy and stability of 0.5%. Details of the rate-calibration technique appear elsewhere.[17]

Film densities were determined by assuming that the sample consists of an amorphous mixture of hard spheres. The Xe packing fraction was assumed to be 0.45.[18] Based upon the optical measurements presented here, the packing fraction of amorphous Cs is determined to be ~0.40. In general the density of binary mixtures is influenced by the relative hard-sphere diameters of the two components,[19] but since the r_{Xe}/r_{Cs} ratio is about 0.8, the correction is small and was ignored. Details concerning the cryogenic and vacuum systems are described elsewhere.[17] UHV standards were maintained throughout this investigation. A description of the substrate assembly is found in Ref. 17.

B. Electrical measurements

The experimental setup was designed to detect a range of conductivities exceeding six orders of magnitude. Mixtures were grown until surface effects became negligible, indicating that the measured conductivities were bulk values. A standard four-probe technique with vapor-deposited Cr electrodes on the sapphire sample substrate was used.

C. Optics

Phase-sensitive detection was used to determine the optical transmission of a chopped light beam (220 Hz) through the mixture which was grown on the sapphire substrate. We employed a technique by which first the transmission through the bare substrate and subsequently through each of several thicknesses of a fixed composition mixture was measured. The film thicknesses required to give sufficient optical absorption ranged from a few thousand angstroms for a pure Cs sample to a few microns for the very dilute Cs mixtures. Near-infrared and optical-energy photons were provided by a tungsten-halogen lamp and dc power supply with a light-intensity stability of 0.1%. The ultraviolet energy photons were from a D_2 lamp and power supply with an intensity stability of 1%. A photomultiplier tube and a tandem Si diode-PbS detector were used to measure the light intensities. The light was dispersed by a double-grating Jarrell-Ash $\frac{1}{4}$-meter monochromator. The electrical conductivity was monitored during the optical measurements as each successive layer was grown as a check of the composition control. For the dilute samples of Cs in Xe a simple double-beam experiment was arranged whereby the intensity of the light passed through the samples was normalized by the incident-light intensity with the use of a homebuilt analog divider.

D. Optical data analysis

A model consisting of two to four classical oscillators was used to extract the optical constants from the data.[20] The parameters in the model are the high-energy dielectric constant and the strength, frequency, and width of each oscillator. These parameters are iteratively adjusted by a computer until the optical transmission predicted by the model (including the effect of the mixture-substrate interface) match the data within a relative error of 5% or less. No physical significance is placed upon the specific values of the parameters of the model. The model serves only as a convenient means of obtaining the optical constants.[17]

III. RESULTS

A. dc conductivity

Shown in Fig. 1 are the dc conductivities of Cs-Xe mixtures. The values extend over approximately 5 orders of magnitude and diverge sharply beyond the measurement capability at the Cs atomic fraction $X = 0.23$. At increasingly larger values of X

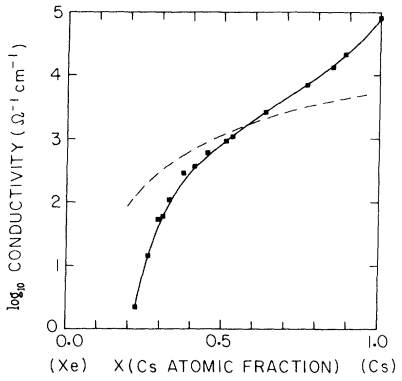

FIG. 1. The dc conductivity of amorphous Cs-Xe mixtures (■) and of expanded fluid (Ref. 49) Cs (---) vs X. The conversion from the density scale of the fluid to the solid mixture composition scale X is discussed in the text.

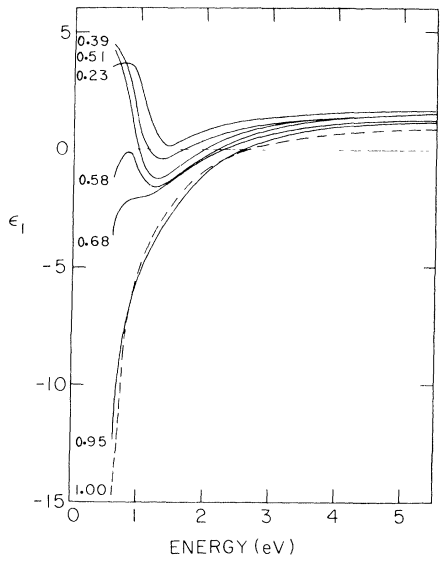

FIG. 2. The real part of the dielectric constant ϵ_1 of Cs-Xe mixtures as a function of photon energy for several compositions. The numbers near each curve represent the Cs atomic fraction X.

the conductivity rises monotonically and for $X > 0.4$, the rise is approximately one order of magnitude per 25 at. % Cs.

No quantitative results on the temperature dependence of the conductivity can be presented as the Cs-Xe mixtures are not sufficiently stable to temperature changes. Pure amorphous Cs layers exhibit a small negative temperature coefficient, $d\ln\sigma/dT = -5.5\times10^{-3}\ \mathrm{K}^{-1}$ between 5 and 10 K. Cs-Xe mixtures in the composition range $0.22 < X < 0.51$ ($2 < \sigma < 10^3\Omega^{-1}\ \mathrm{cm}^{-1}$) exhibit positive temperature coefficients of the order of $10^{-2}\ \mathrm{K}^{-1}$. However, the conductivity changes were only partly reversible in the temperature range 5–10 K, and the composition dependence was not easily reproducible. In the intermediate range $0.5 < X < 0.9$ the temperature coefficient was too small to be measured ($d\ln\sigma/dT < 3\times10^{-4}\ \mathrm{K}^{-1}$).

B. Optical Properties ($0.2 < X < 1$)

The real part of the dielectric constant (ϵ_1) is plotted in Fig. 2. The composition range separating metallic mixtures, in which $\epsilon_1(\hbar\omega\to0) < 0$, from nonmetallic mixtures is $0.50 < X < 0.58$. A flat high-energy region contrasts with the region near 1.2 eV where most of the absorption in these mixtures occurs. The 1.2-eV absorption feature is also prominent in the optical conductivity (Fig. 3). The peak height progressively increases with increasing Cs content, reaching a maximum at $X = 0.51$, then decreases monotonically as $X = 1$ is approached.

A monotonic energy shift of the optical-conductivity maximum by a total of 0.25 eV towards lower energy is observed over the composition range $0.15 < X < 0.51$.

An optical-energy gap may be extracted from the linear extrapolation toward low photon energies of the function $\sqrt{\epsilon_2}\hbar\omega$ vs $\hbar\omega$,[21] where ϵ_2 is the ima-

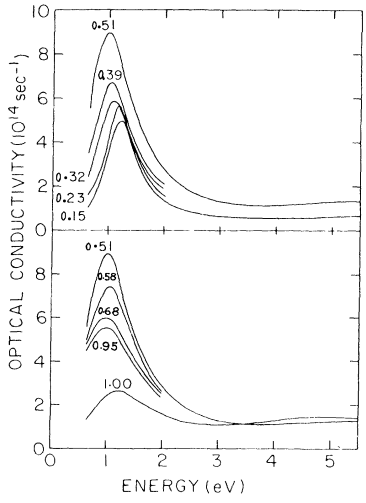

FIG. 3. The optical conductivity of Cs-Xe mixtures vs photon energy for several compositions. The numbers near each curve represent the Cs atomic fraction X.

ginary part of the dielectric constant. Figure 4 contains several plots of this function for compositions in the range $0.15 < X < 0.6$. Experimental data points are indicated, and over the energy range where this function is linear, a best-fit line is drawn and extrapolated to the energy axis. Each point of intersection (the energy gap) is plotted as a function of the corresponding composition X in the inset graph of Fig. 4. The magnitude of the gap decreases monotonically with increasing X and closes between 0.51 and 0.58 at. fraction Cs.

In Fig. 5, ϵ_1 at 0.65 eV is plotted as a function of composition. From a value of 1.7 for Xe, ϵ_1 increases with increasing X to a peak of 5.6 at $X = 0.49$. At $X = 0.52$, ϵ_1 decreases sharply and changes sign at $X = 0.55 \pm 0.01$, followed by a monotonic decrease to more negative values.

A significant difference exists between the optical properties of the pure Cs sample and the $X = 0.95$ mixture (Fig. 3). The pure Cs sample has a maximum at 1.2 eV of one-half the value of the maximum of the $X = 0.95$ mixture which is centered at 1.0 eV. The significance of the differences in the optical properties will be discussed in Sec. V.

C. Optical properties of dilute mixtures

Figure 6 contains the extinction coefficient $a^{-1} \ln(I_0/I)$ for several compositions where a is the sample thickness, I_0 the light intensity before the sample deposition, and I the light intensity after the sample deposition.

At the lowest concentration measured

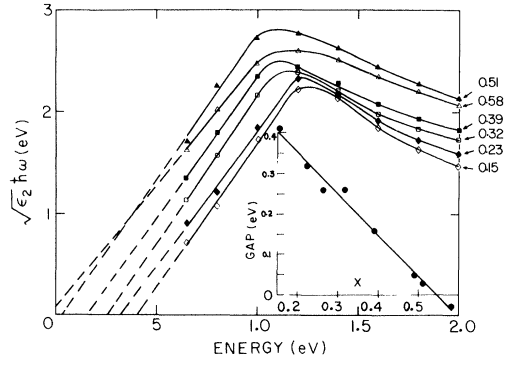

FIG. 4. The function $\sqrt{\epsilon_2}\hbar\omega$ vs photon energy and the inset graph of the optical gap (see text) vs the composition X(●). The function ϵ_2 is the imaginary part of the dielectric constant of Cs-Xe mixtures.

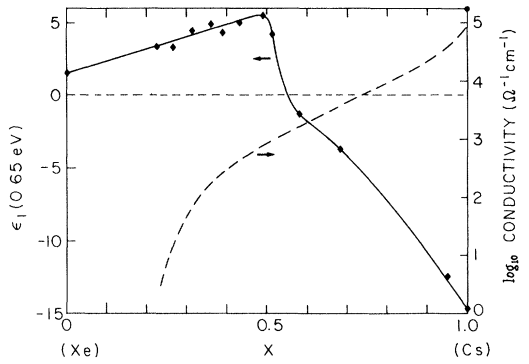

FIG. 5. The real part of the dielectric constant ϵ_1 at 0.65 eV (◆) and the dc conductivity (---) vs composition X.

($X = 0.0032$), two strong spectral features at 1.35 and 1.75 eV are evident. We assign them as the Cs_2 ($A \leftarrow X$) and ($B \leftarrow X$) molecular bands on the basis of a comparison with the gas-phase band envelope expected for Cs_2 at 6 K.[22] Li_2 and Na_2 molecular bands show very small matrix shifts when compared to the gas-phase band systems.[23,24] The small feature at 1.45 eV is assigned as belonging to the Cs atomic $6^2P_{3/2,1/2} \leftarrow 6^2S_{1/2}$ transition. Weyhmann and Pipkin[6] have previously measured transmission spectra of Cs atoms in Xe at higher dilution ($X = 0.001$) and find the typical alkali atom "triplet" with components at 1.44, 1.39, and 1.34 eV. In our case, the two latter low-energy components are presumably covered by the much stronger Cs_2 ($A \leftarrow X$) band.

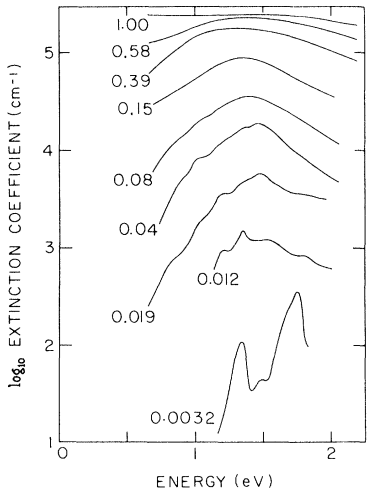

FIG. 6. The logarithm of the extinction coefficient vs photon energy for several compositions. The Cs atomic fraction X is indicated for each composition.

At slightly higher Cs concentration ($X = 0.012$) both atomic and dimer absorptions have disappeared. Discrete absorption bands presumably belonging to small Cs_X clusters are superimposed on a broad baseline absorption. This broad absorption is apparent even in the very dilute mixture ($X = 0.0032$) and is also evident in the spectrum shown by Weyhmann and Pipkin (Fig. 3 of Ref. 6). The magnitude of the broad absorption grows monotonically with X and the maximum shifts in energy from 1.5 to 1.35 eV over the composition range $X = 0.003 - 0.15$.

IV. THEORETICAL MODELS

A. The Mott transition in homogeneous systems

One theoretical approach to the explanation of the MNMT is attributed to Mott.[7,25] Mott considers a system which is a microscopically homogeneous material. The MNMT is a quantum-mechanical phenomenon whereby the system has a metallic density of states on the metallic side of the transition and a very low density of states (or localized states) at the Fermi energy on the nonmetallic side. Mott argues that when the system is near the MNMT, a local minimum in the density of states (pseudogap) exists at the Fermi energy. Under certain conditions, depending primarily upon the state of the disorder in the system,[26] the states at the Fermi energy are localized and the electrical transport properties at low temperature are governed by hopping conduction between localized states (variable range hopping). Mott predicts[7] the temperature (T) dependence of the conductivity for such a mechanism to be a power law in $T^{-0.25}$.

A feature which emerges from the Mott transition is that at $T = 0$ a discontinuous change of the conductivity occurs at the MNMT. Mott proposed the concept of the minimum metallic conductivity ($\sigma_{\min}$) which is the source of the discontinuity.[7] The value of $\sigma_{\min}$ occurs when the Fermi energy is at the mobility edge, i.e., at that energy which separates the density of states into two regions with different character: (1) where the states are extended and (2) where the states are localized or do not exist. When the Fermi energy lies in the region where extended states exist, metallic transport occurs and is finite at $T = 0$. When the Fermi energy lies within another region the transport is activated and therefore is zero at $T = 0$. Mott places the value of $\sigma_{\min}$ at $0.026\ e^2/\hbar a$, where a is the atomic separation.[27] Mott admits that the constant 0.026 may be wrong by a factor of two either way,[25,26] but $\sigma_{\min}$ generally is the range $100 - 1000\ \Omega^{-1}\,\mathrm{cm}^{-1}$.

Within the Mott picture a discontinuous change in the optical properties also is expected.[28] In a system of free electrons ϵ_1 decreases monotonically with decreasing photon energy (E) and is negative for energies smaller than the plasma frequency energy. A nonmetallic system characteristically has positive values of ϵ_1 as $E \to 0$, so that a discontinuous transition (polarization catastrophe) from the metallic to nonmetallic state is reflected in $\epsilon_1(E \to 0)$. Furthermore, as the transition is approached from the nonmetallic side, $\epsilon_1(0)$ increases before the discontinuous decrease occurs at the transition.[29] Viewed in terms of an optical gap, the closing of the energy gap (Fig. 4) leads to an inverse-square divergent increase of $\epsilon_1(0)$ with the gap energy.[30] Having summarized the properties of homogeneous materials at the MNMT, the behavior of inhomogeneous materials is discussed next.

B. The MNMT in inhomogeneous systems

A second mechanism which can produce an MNMT is classical percolation in microscopically inhomogeneous systems.[25,31,32] The model is a system consisting of well-defined metallic and insulating regions, each characterized by bulk physical parameters. In the continuous classical percolation scheme a composition parameter (C is the metallic volume fraction) characterizes the material. For values of C close to zero the material primarily consists of insulator-surrounding isolated metallic clusters. As C is increased the number and size of the clusters increase, and smaller clusters combine to form larger metallic regions. At $C = C^*$ (the percolation threshold) the material contains enough metal to form a continuous metallic pathway across the sample, enabling electronic transport to commence.

In the case of continuous classical percolation $C^* = 0.145$.[33] An effective-medium theory (EMT) has been developed by Jortner and Cohen to describe several physical properties as a function of C.[31,34] In the vicinity of C^* the assumptions of EMT are not valid, and numerical simulations are required to provide the functional dependence of transport properties on C.[33,36] From the numerical simulations a critical exponent (b) for the conductivity $\sigma \propto (C - C^*)^b$ is obtained, $b = 1.6 \pm 0.1$. Thus a quantitative means of determining the appli-

cability of percolation theory to physical systems is available from the behavior of the conductivity.

The theoretical optical behavior of inhomogeneous systems has been studied from the point of view of EMT.[37] The numerical simulations indicate that for $0 < C < C^*$, $\epsilon_1(E = 0)$ increases with increasing C followed by an abrupt decrease at C^*. Subsequent increases in C produce increasingly negative values of $\epsilon_1(0)$.

C. Dilute systems

The optical response of systems containing minute quantities of metal is sensitive to, among other factors, the metallic distribution. A material with a given composition can consist of isolated atoms in the insulating matrix, or of clusters of atoms containing any number of atoms. In the first instance atomic and molecular absorption peak heights exhibit a specific composition dependence according to the matrix coordination number and distribution statistics. In the second case, a theory of optical scattering from metallic grains embedded in an insulating material, the Maxwell-Garnett theory (MGT),[38] is appropriate. A notable consequence of this theory is the prediction of a Mie resonance. In the dilute composition range the location of the Mie resonance is at the energy (E^R) which satisfies the relation $\epsilon_1^M(E^R) = -2\epsilon_1^I(E^R)$, where M denotes metal and I denotes insulator. The MGT predicts a progressively larger red shift in the center frequency of the resonance with increasing metallic content. Further discussion of the MGT will be included in the next section.

V. DISCUSSION

A. Metallic distribution

As pointed out in Sec. III the Cs-Xe mixtures are structurally unstable upon increases in temperature. That structural changes occur is inferred from the partly irreversible response of the conductivity to thermal cycling. The conductivity increases with increasing temperature, implying that either the density increases or metallic clustering occurs or some combination of the two phenomena is involved.

In order to test the hypothesis that preferential clustering occurs in Cs-Xe mixtures, the granular cluster model (MGT) described in Sec. IV was used. Shown in Fig. 7 is ϵ_1 according to the MGT where the optical parameters appropriate for amorphous Xe and for amorphous Cs (see following subsection) have been applied to the model. Qualitatively the trend with decreasing Cs content is the same as that for the data (Fig. 2).

In particular the presence and location of the minimum in ϵ_1 for several compositions are comparable. A trend to shift the location of the minimum to higher energies with decreasing Cs content is apparent in both Figs. 2 and 7. Qualitative similarities between the data and MGT also occur in the optical conductivity. The presence of a maximum which shifts toward lower energy with increasing Cs content is seen in the Xe-rich compositions. This maximum (according to MGT) is associated with the Mie resonance phenomena in dilute granular metal systems.[39] The location of the resonance (E^R) is determined from the solution to the equation $\epsilon_1^{Cs}(E^R) = -2\epsilon_1^{Xe}(E^R)$. This equation is satisfied at $E^R = 1.35$ eV. The proximity of the maximum in each extinction-coefficient (α) curve for dilute mixtures (Fig. 6) to this value is indicative of the possible applicability of the model. In Fig. 8 the comparison of α is made between the data and MGT at $X = 0.012$. Although the MGT result is normalized by a factor of 13, the location of the maximum at 1.52 eV and the half-width of 0.7 eV are comparable with the data for which the location of the maximum is 1.46 eV and the half-width is 0.8 eV. Numerical modeling of the optical properties based upon EMT did not produce results with a good correspondence to the data.

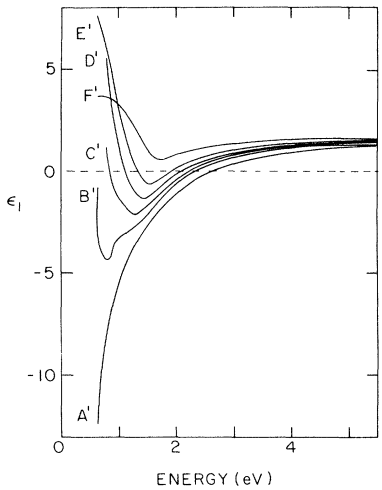

FIG. 7. The real part of the dielectric constant ϵ_1 of Cs-Xe mixtures obtained from Maxwell-Garnett granular-cluster theory vs photon energy for several compositions. $A' : C = 1.0$ ($X = 1.00$), $B' : C = 0.7$ ($X = 0.54$), $C' : C = 0.6$ ($X = 0.43$), $D' : C = 0.5$ ($X = 0.33$), $E' : C = 0.4$ ($X = 0.25$), $F' : C = 0.2$ ($X = 0.11$).

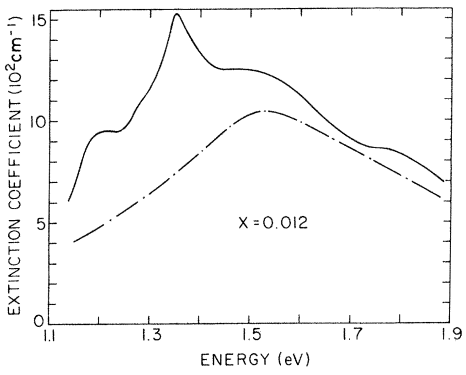

FIG. 8. The extinction coefficient for the composition $X = 0.012$ (———) and the Maxwell-Garnett result $\div 13$ (—·—·) vs photon energy.

The apparent dilemma of the dilute Cs-Xe mixtures exhibiting properties compatible with a model of large clusters and simultaneously with optical features of small clusters, is resolved by an examination of Fig. 8. In order to provide a comparable fit of the data with the results of MGT, it is necessary to reduce the MGT values of α by a factor of 13. Interpreting this as meaning that the dilute Cs-Xe mixtures contain only 8 at. % of the Cs in the form of metallic grains, then the remaining Cs may be present as a distribution of small clusters with discrete optical-absorption properties distinct from macroscopic behavior.

B. Metal-nonmetal transition

Of critical importance to the comparison of Cs-Xe mixtures to an inhomogeneous model with respect to the MNMT is the determination of the metallic volume fraction (C) scale relative to the composition scale X. Attention must be paid to the underlying assumptions concerning how the atoms in the mixture are packed. The validity of our use of the hard-sphere model and a packing fraction of 0.45 (Ref. 18) for Cs is supported by the present optical data. A significant difference between the optical properties of the pure Cs ($X = 1$) and the $X = 0.95$ samples is most apparent in Fig. 3. A relatively large change in conductivity between these two compositions is also notable. We attribute this distinctly different character between these almost identical (compositionwise) samples as being a result of structural differences. Corroborative evidence is the irreversible behavior of the conductivity with temperature. The conductivity of each mixture increases irreversibly with increased temperature from which structural shrinkage can be inferred.

We assume a modified free-electron model of the form[40] $\epsilon_1 = 1 + \epsilon_c - (\omega_p/\omega)^2 + \epsilon_i$, where ϵ_c is the core polarizability, ω_p is the plasma frequency ($\omega_p^2 = 4\pi ne^2/m^*$), and ϵ_i is a correction term resulting from interband transitions. The effective mass is m^* and the free-electron density is n. If ϵ_i is small and only the energy range $E << \hbar\omega_p$ is examined then ω_p^2 is determined from the low-frequency slope of ϵ_1 as a function of $-\omega^{-2}$. In fact for Cs in the infrared region of the spectrum, ϵ_i represents a correction which produces an apparent decrease in ω_p^2 of 9%.[41] Ignoring the term ϵ_i, the values of $\hbar\omega_p$ measured from the present data at $X = 0.95$ and 1.0 are 2.27 and 2.56 eV, respectively. The value for polycrystalline Cs is 3.0 eV.[41,42] Assuming m^* is constant in these three samples, ω_p determines the value of n which in the free-electron model determines also the mass density or hard-sphere packing fraction f of each sample ($f = 0.68$ for the bcc structure of crystalline Cs). The values of f which result are 0.40 and 0.50 for $X = 0.95$ and 1.0, respectively, indicating that both our pure Cs sample and the $X = 0.95$ sample are significantly less dense than polycrystalline Cs. Perhaps it is surprising that the addition of only 5 at. % Xe decreases the density significantly from the $X = 1.0$ value and stabilizes the amorphous state, but similar behavior was observed in Hg-Xe as well.[43] In light of the fact mentioned above that interband transitions tend to indicate a spuriously low value of ω_p^2 (i.e., if the term ϵ_i is ignored) and in light of the analysis above from which $\omega_p^2 \propto f$ within the hard-sphere model, the value $f = 0.40$ determined from the data is in agreement with the accepted value 0.45 for amorphous packing of hard spheres. Thus the value 0.45 was used in this study.

These criteria concerning the mixture densities enable the establishment of the metallic volume fraction (C) scale. The dc conductivity is replotted in Fig. 9 as a function of C. A best-fit line to the relation $\sigma \propto (C - C^*)^b$ also is drawn where $C^* = 0.32 \pm 0.01$ and $b = 3.3 \pm 0.1$. Another investigation of the Cs-Xe system indicated a stronger divergence in the dc conductivity near the same composition.[3] The discrepancy between the value in the data and the value dictated by percolation

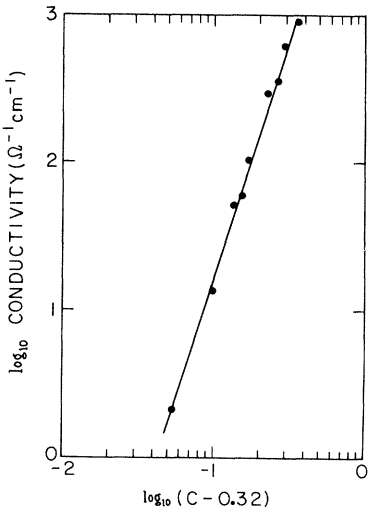

FIG. 9. The dc conductivity (●) vs $C - 0.32$. The metallic volume fraction C for amorphous Cs-Xe mixtures is defined in the text.

theory ($b = 1.6$) is sufficiently great to exclude percolation as the controlling mechanism of the MNMT in Cs-Xe mixtures. As the theoretical value for C^* depends on the clustering behavior of the metal, the difference between the measured $C^* = 0.32$ and the theoretical $C^* = 0.145$ (for no clustering correlation) is less significant than the difference in b.

The data in Fig. 5 indicate unambiguously that the MNMT is located at $X = 0.55 \pm 0.01$, where the low-energy value of ϵ_1 changes sign as a function of composition. Qualitatively the composition dependence follows the behavior predicted by both EMT and Mott, whereby from $X = 0$ to the MNMT $\epsilon_1(0)$ rises monotonically followed by a sharp drop at the transition and a subsequent monotonic decrease toward $X = 1$. That the percolation picture does not describe Cs-Xe mixtures is evident from the location of the transition at $X = 0.55$ corresponding to $C^* = 0.32$, instead of $C^* = 0.145$ dictated by percolation theory. The dc conductivity at the MNMT is about 1000 $\Omega^{-1}\,\mathrm{cm}^{-1}$, which is compatible with the accepted range of values for Mott's $\sigma_{\min}$.[26]

The optical gap, which was determined according to the prescription contained in Sec. III, is shown in Fig. 4. The gap decreases with increasing Cs content and a corresponding increase of ϵ_1 (0.65 eV) (Fig. 5) is apparent. Such behavior is described qualitatively by a simple two-band model[30] whereby as the gap approaches zero, the value of $\epsilon_1(0)$ increases according to the inverse square of the gap energy. However, a divergence is not apparent in Fig. 5. The closure of the optical gap occurs at $X = 0.545 \pm 0.01$.

The meaning of an optical gap in an amorphous semiconductor has been discussed by many authors including Mott[7] and Tauc.[44] The term pseudogap is currently used in connection with the MNMT. Basically the difference between a true optical gap and a pseudogap is that localized states exist within the pseudogap at the Fermi energy and are absent in an optical gap. Thus a system with a pseudogap exhibits two optical excitation thresholds as the MNMT is approached from the nonmetallic side. One is the true optical gap which exists far from the transition in which no localized states exist at the Fermi energy. The other is the mobility gap which persists after the optical gap has closed, as long as the states at the Fermi energy remain localized. From the coincidence of the closure of the optical gap (Fig. 4) and the onset of extended-state (metallic) properties (Fig. 5) at virtually the same composition, the composition range over which localized states exist at the Fermi energy is very narrow in Cs-Xe mixtures. Similar behavior is exhibited at the MNMT in Cs-Sb amorphous mixtures in which localization occurs within a narrow composition range.[45] Examples of systems for which a finite composition range exists in which the states are localized at the Fermi energy are mixtures of amorphous solid[17] and of liquid[46] Cs and Au.

It is worthwhile to note that a comparison can be made between expanded liquid Cs data[9,47,48] and the low-temperature analog Cs-Xe mixtures. Assuming a direct correspondence between the mass density of the expanded liquid and the effective Cs density in the Cs-Xe mixtures, then the density[47] (0.43 $\mathrm{g\,cm}^{-3}$) associated with the density at the critical temperature of the expanded liquid corresponds to the composition $X = 0.21$. This is the location of the divergence of the conductivity with composition in Cs-Xe mixtures. The conductivity[49] of the expanded fluid Cs appears in Fig. 1. Recently published magnetic susceptibility data[48] on expanded fluid Cs indicate that the MNMT occurs at a density of 0.8 $\mathrm{g\,cm}^{-3}$ with an associated conductivity of 1000 $\Omega^{-1}\,\mathrm{cm}^{-1}$. The composition associated with this density in the Cs-Xe mixtures is $X = 0.48$ where the conductivity is 800 $\Omega^{-1}\,\mathrm{cm}^{-1}$, while the MNMT in the Cs-Xe mixtures occurs at $X = 0.55$ where the conductivity is 1300 $\Omega^{-1}\,\mathrm{cm}^{-1}$. Thus the van der Waals bond in the Cs-Xe mixtures is not passive but shifts the MNMT to higher densities of Cs relative to the den-

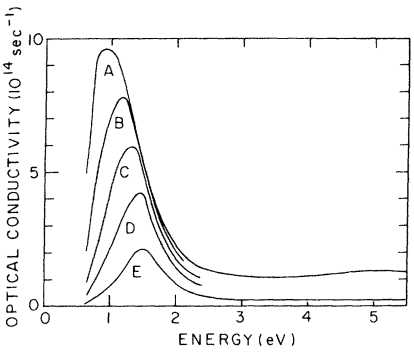

FIG. 10. The optical conductivity of Cs-Xe mixtures obtained from Maxwell-Garnett granular-cluster theory vs photon energy for several compositions. $A:C=0.5$ ($X=0.33$), $B:C=0.4$ ($X=0.25$), $C:C=0.03$ ($X=0.18$), $D:C=0.2$ ($X=0.11$), $E:C=0.1$ ($X=0.05$).

sity at which the MNMT occurs in the expanded fluid (similar to what is found in Hg-Xe mixtures[43]).

In summary the following points are made concerning the results of this work.

(1) Cs-Xe mixtures prepared by codeposition at 6 K are amorphous with a characteristic hard-sphere packing fraction of about 0.45, as determined from the optical data.

(2) The mixtures are structurally unstable to increases in temperature as evidenced by partial irreversibility of the dc conductivity to thermal cycling.

(3) The dc conductivity indicates that an MNMT occurs as a function of composition. The measurable conductivity range spans about five orders of magnitude from the value for metallic Cs through Mott's σ_{min} to the insulating Xe-rich mixtures.

(4) In dilute mixtures of Cs in Xe, evidence based upon the optical data is presented for a spatial distribution scheme of Cs in which most of the Cs is distributed randomly on the microscopic scale while a small amount exists in the form of metal grains. The tendency of the dc conductivity to increase with temperature increases is consistent with preferential cluster formation.

(5) Qualitatively the trends in the optical data with composition follow those predicted from the granular-metal Maxwell-Garnett theory (Fig. 10), including the presence of a Mie resonance.

(6) We have demonstrated, based upon the behavior of the dc conductivity and optical data with the Cs volume fraction, that although preferential clustering occurs, it is not sufficiently prominent to apply the model of classical percolation theory.

(7) The MNMT is characterized by the closure of the optical gap on the nonmetal side of the transition and the appearance of free-electron-type optical behavior on the metallic side separated by a very narrow (possibly zero) region in composition at 0.55 ± 0.01, in which the states at the Fermi energy are localized.

(8) A polarization catastrophe of the Mott type of $\epsilon_1(0)$ with composition is not evident. Instead a more gradual drop occurs at the MNMT.

(9) The value of the dc conductivity at the transition is 1300 $\Omega^{-1}\,\mathrm{cm}^{-1}$, which lies within the range of acceptable values of Mott's minimum metallic conductivity.

(10) The van der Waals interaction of Cs with Xe is significant when comparing these mixtures to the high-temperature expanded fluids. In addition the nonpassive role of Xe in Cs-Xe mixtures is evident in the optical properties which reveal atomic and molecular line shifts and a broad Mie resonance.

ACKNOWLEDGMENTS

S.L. wishes to acknowledge a postdoctoral fellowship from the Stiftung fuer Stipendien auf dem Gebiet der Chemie, Basel. This work was supported by the U.S.-Israel Binational Science Foundation and the Basic Research Division of the Israel Academy of Science. R.D.S. wishes to thank O. Cheshnovski for his help during the course of this work.

*Present address: Bell Laboratories, 600 Mountain Ave., Murray Hill, N. J. 07974.

[1]B. Raz, A. Gedanken, U. Even, and J. Jortner, Phys. Rev. Lett. 28, 1643 (1972).

[2]O. Cheshnovski, U. Even, and J. Jortner, Solid State Commun. 22, 745 (1977).

[3]R. Avci and C. P. Flynn, Phys. Rev. B 19, 5967 (1979).

[4]R. C. Cate, J. G. Wright, and N. E. Cusack, Phys. Lett. 32A, 467 (1970).

[5]D. J. Phelps and C. P. Flynn, Phys. Rev. B 14, 5279 (1976).

[6]W. Weyhmann and F. M. Pipkin, Phys. Rev. 137, 490

(1965).
[7]N. F. Mott, *Metal-Insulator Transitions* (Taylor and Francis, London, 1974).
[8]U. Even and J. Jortner, Philos. Mag. 25, 715 (1972).
[9]F. Hensel, Can. J. Chem. 55, 2225 (1977).
[10]A. Menth, E. Buehler, and T. H. Geballe, Phys. Rev. Lett. 22, 295 (1969).
[11]W. D. Straub, H. Roth, W. Bernard, S. Goldstein, and J. E. Mulhern, Phys. Rev. Lett. 21, 752 (1968).
[12]R. D. Swenumson, U. Even, and J. C. Thompson, Philos. Mag. 37, 311 (1978).
[13]B. I. Halperin and T. M. Rice, in *Solid State Physics,* edited by H. Ehrenreich, F. Seitz, and D. Turnbull (Academic, New York, 1968), Vol. 21, p. 115.
[14]J. C. Thompson, *Electrons in Liquid Ammonia* (Clarendon, Oxford, 1976).
[15]W. Schulze and D. H. Kolb, Faraday Discuss. Chem. Soc. 70, 1098 (1974).
[16]R. D. Swenumson and U. Even, Rev. Sci. Instrum. 52, 559 (1981).
[17]R. D. Swenumson and U. Even, Phys. Rev. B 24, 5743 (1981), paper III.
[18]N. W. Ashcroft and J. Lekner, Phys. Rev. 145, 83 (1966).
[19]W. M. Visscher and M. Bolsterli, Nature 239, 504 (1972).
[20]H. W. Verleur, J. Opt. Soc. Am. 58, 1356 (1968).
[21]M. L. Theye, in *Proceedings of the 5th International Conference on Amorphous and Liquid Semiconductors,* edited by J. Stuke and W. Brenig (Taylor and Francis, London, 1974),
[22]K. P. Huber and G. Herzberg, *Constants of Diatomic Molecules* (Van Nostrand Reinhold, New York, 1979).
[23]L. Andrews and G. C. Pimentel, J. Chem. Phys. 47, 2905 (1967).
[24]M. Hofmann, S. Leutwyler, and W. Schulze, Chem. Phys. 40, 145 (1979).
[25]*The Metal Nonmetal Transition in Disordered Systems,* edited by L. R. Friedman and D. P. Tunstall (SUSSP, Edinburgh, 1978), p. 479.
[26]N. F. Mott, Philos. Mag. 13, 989 (1966).
[27]N. F. Mott and E. A. Davis. *Electronic Properties of Noncrystalline Materials,* 2nd ed. (Oxford, London, 1978).
[28]N. F. Mott, Philos. Mag. B 37, 377 (1978).
[29]O. Cheshnovsky, U. Even, and J. Jortner, unpublished.
[30]J. C. Phillips, Rev. Mod. Phys. 42, 317 (1970).
[31]J. Jortner and M. H. Cohen, Phys. Rev. B 13, 1548 (1976).
[32]S. Kirkpatrick, Phys. Rev. Lett. 27, 1722 (1971).
[33]S. Kirkpatrick, Rev. Mod. Phys. 45, 574 (1973).
[34]I. Webman, J. Jortner, and M. H. Cohen, Phys. Rev. B 11, 2885 (1975).
[35]I. Webman, J. Jortner, and M. H. Cohen, Phys. Rev. B 15, 1936 (1977).
[36]R. D. Swenumson and J. C. Thompson, Phys. Rev. B 14, 5142 (1976).
[37]I. Webman, J. Jortner, and M. H. Cohen, Phys. Rev. B 15, 5712 (1977).
[38]J. C. Maxwell-Garnett, Philos. Trans. Soc. London 203, 385 (1904); 205, 237 (1906).
[39]J. I. Gittleman and B. Abeles, Phys. Rev. B 15, 3273 (1977).
[40]M. H. Cohen, Philos. Mag. 3, 762 (1958).
[41]N. V. Smith, Phys. Rev. B 2, 2840 (1970).
[42]T. Hanyu and S. Yamaguchi, J. Phys. Soc. Jpn. 37, 994 (1974).
[43]O. Cheshnovsky, U. Even, and J. Jortner, Phys. Lett. A 71, 255 (1979).
[44]J. Tauc, in *Optical Properties of Solids,* edited by F. Abeles (North-Holland, Amsterdam, 1970), p. 277.
[45]R. D. Swenumson and U. Even, Phys. Rev. B 24, 5736 (1981), paper II.
[46]R. Dupree, D. J. Kirby, W. Freyland, and W. W. Warren, Phys. Rev. Lett. 45, 130 (1980).
[47]I. G. Dillon, P. A. Nelson, and B. S. Swanson, J. Chem. Phys. 44, 4229 (1966).
[48]W. Freyland, Phys. Rev. B 20, 5104 (1979).
[49]W. Freyland, H. P. Pfeifer, and F. Hensel, in *Proceedings of the Fifth International Conference on Amorphous and Liquid Semiconductors,* edited by J. Stuke and W. Brenig (Taylor and Francis, London, 1974), p. 1327.